Journal of Power Sources 250 (2014) 212–219

Contents lists available at ScienceDirect

Journal of Power Sources

journal homepage: www.elsevier.com/locate/jpowsour

Improved coking resistance of direct ethanol solid oxide fuel cells with a Ni–S_x anode

Ning Yan, Jing-Li Luo*, Karl T. Chuang

Department of Chemical and Materials Engineering, University of Alberta, Edmonton, Alberta T6G 2G6, Canada

HIGHLIGHTS

- Ni–S_x anode was developed via in-situ H_2S treatment at elevated temperature.
- SOFC employed with Ni–S_x anode exhibited good coking resistance in ethanol.
- S species on Ni reduced the rate of both coke formation and Ni metal dusting.

ARTICLE INFO

Article history:
Received 29 August 2013
Received in revised form
24 October 2013
Accepted 2 November 2013
Available online 18 November 2013

Keywords:
Direct ethanol solid oxide fuel cell
Ni–S_x anode
In-situ H_2S treatment
Ethanol–CS_2 mixture
Coke resistance

ABSTRACT

In this study, the coking resistance of anode supported direct ethanol solid oxide fuel cell with a Ni–S_x anode was investigated comparatively with the conventional cell using pure Ni catalyst. The surface catalytic properties of Ni were manipulated via depositing a layer of S atoms. It was confirmed that on the surface of Ni, a combination of S monolayer and elemental S was formed without producing Ni_3S_2 phase. The developed Ni–S_x cell exhibited a significantly improved coke resistivity in ethanol feed while maintaining an adequately high performance. The S species on Ni enabled the suppression of the coke formation as well as the alleviation of the metal dusting effect of the anode structure. After operating in ethanol fuel for identical period of time at 850 °C, a maximum power density of 400 mW cm^{-2} was sustained whereas the conventional cell performance decreased to less than 40 mW cm^{-2} from the original 704 mW cm^{-2}. In an optimized stability test, the Ni–S_x cell operated at 750 °C for more than 22 h until the fuel drained without any degradation.

© 2013 Elsevier B.V. All rights reserved.

1. Introduction

Solid oxide fuel cell (SOFC) is capable of converting a variety of hydrocarbon fuels into electricity directly via electrochemical reactions, which has been intensively studied as one of the future power generation techniques [1–3]. Among all the commercial feedstock available for SOFC, including fossil fuels derived hydrogen and natural gas, ethanol has drawn increasing attentions as the SOFC feed since it is practically produced from renewable biomass [4–6]. Added attractiveness of ethanol also includes the convenience-safety during its transportation-storage. Handling this low-toxic liquid is apparently easier than gaseous fuels, especially in the application of portable or compact SOFC power unit.

However, the commonly used Ni anode catalyst in conventional SOFC readily catalyzes the formation of coke in hydrocarbon fuels, which necessitates the incorporation of an additional external steam reformer attached to the fuel cell system. To reduce the system complexity, SOFC with the internal steam reforming process has been developed and alternative methodology has been employed, aiming at minimizing the coking effects. In general, the optimization of SOFC operation parameters including C/steam ratio of the feed and fuel utilization was considered as one method to accomplish the objective [7]. The other method focused on the design and development of coke tolerant anode candidates such as using bimetallic alloys and ceramic composites [4,8–10]. Nevertheless, their performances are not comparable with Ni in terms of either catalytic activity or economic feasibility.

H_2S is usually recognized as a detrimental poison agent in SOFC [11,12]. However, it was reported that the H_2S treated transition metals such as Ni and Fe, were more resistant against coking and metal dusting [13–15]. Herein, we take the advantage of the H_2S treatment to manipulate the surface property of Ni catalyst in the direct ethanol SOFC. The electrochemical performances and coking

* Corresponding author. Tel.: +1 780 492 2232; fax: +1 780 492 2881.
E-mail address: Jingli.Luo@ualberta.ca (J.-L. Luo).

0378-7753/$ – see front matter © 2013 Elsevier B.V. All rights reserved.
http://dx.doi.org/10.1016/j.jpowsour.2013.11.002

resistance of the cell before and after S introduction were studied; the employed Ni–S_x anode was also characterized.

2. Experimental

2.1. In-situ H_2S treatment and ethanol fuel preparation

The fabrication of the anode supported SOFC button cell with a Ni–YSZ (yttria-stabilized zirconia) composite anode was detailed in our previous work described elsewhere [16]. The YSZ electrolyte, the Ni–YSZ functional layer and the LSM ($La_{0.8}Sr_{0.2}MnO_{3-x}$)–YSZ cathode layers were applied onto the anode substrate via spin coating method. During fuel cell test, the set-up was heated up to 850 °C in the furnace. Then, a stream of 10% H_2 balanced by N_2 was pumped to the anode chamber to gradually reduce NiO to Ni. When the open circuit voltage (OCV) reached ~1.0 V, the gas was switched to pure H_2 to complete the reduction process until a steady state was achieved. Subsequently, the cell was polarized at 0.8 V for 2 h in order to stabilize its electrochemical performances. To obtain a Ni–S_x anode, the *in-situ* H_2S treatment was performed by feeding a stream of certified 500 ppm $H_2S + H_2$ mixture into the SOFC running at the potentiostatic mode with the applied voltage of 0.8 V. Metal dusting resistance study was carried out using Ni foam (Vale Canada Ltd.) in a quartz tube heated to the specified temperature in a stream of pure CO.

The ethanol–CS_2 mixture was designated to fuel the cell with a Ni–S_x anode. Firstly, the anhydrous ethanol was homogenized with the carbon disulfide (>99. 9%, Fisher Scientific) with a volume ratio of 10^4:1. Then the de-ionized water was slowly dissolved into the ethanol mixture with a volume ratio of 1:2. In the control group, ethanol was directly mixed with water without adding CS_2. The resulting liquid fuel was vaporized in a glass bubbler heated using a water bath adjusted to 70 °C, and a N_2 stream with a flow rate of 10 mL min^{-1} was applied as the carrier gas bringing the humidified ethanol mixture to the SOFC anode chamber.

2.2. Catalyst characterization and fuel cells performance determination

The cross sectional morphologies of the tested button cell were examined using a Hitachi S-2700 scanning electron microscope (SEM) with an energy dispersive X-ray spectrometer (EDS). X-ray photoelectron spectroscopy (XPS) was performed using a Kratos Analytical AXIS 165. A monochromated Al Ka (hv = 1486.6 eV) source was used at a power of 210 W, the base pressure in the analytical chamber was maintained at of 3×10^{-8} Pa. The obtained spectra were analyzed using the Thermo Avantage software referenced to the C 1s binding energy of 285.0 eV. For curve fitting and deconvolution, a shirley-type background subtraction and a Gaussian–Lorentzian peak shape were applied.

Au meshes were used as both the anode and cathode current collectors during fuel cell tests. The active area (cathode) of the button cell was 0.25 cm^2, pure oxygen was used as the oxidant with a flow rate of 50 ml min^{-1}. A gas chromatography (GC) was attached to the anode gas outlet for the analysis of the effluent composition. The current–voltage characteristics were recorded using a Solartron 1287 electrochemical interface. The electrochemical impedance spectra (EIS) were measured at OCV condition with a Solartron 1255B frequency response analyzer, in which an AC amplitude of 10 mV and a frequency range from 0.1 Hz to 100 KHz were employed. After the completion of the test, the set-up was cooled down to room temperature in a pure H_2 atmosphere.

3. Results and discussions

3.1. Ni–S_x anode characterizations

Fig. 1a shows the cross-sectional images of the anode supported SOFC button cell after H_2S treatment. Relative to the conventional cell with a fresh Ni anode, there was not any observable difference in the morphology. The purpose for adding CS_2 was to maintain the S coverage on Ni surface since S chemisorption was partially reversible in the anode environment without H_2S [12,17]. In the effort to detect S species, an EDS elemental analysis was performed within the observed anode area. The obtained spectrum was given in Fig. 1b in which no S signal was recorded. With consideration of the EDS resolution and the vertical depth profile being analyzed on the sample surface (sub-micrometer to micrometer), it was rational to conclude that bulk Ni sulfide was unlikely to form under the experimental condition. After operating in ethanol fuels for 30 min at 850 °C, serious coke formation could be seen on the fresh Ni catalyst in Fig. 2a. In contrast, on the Ni–S_x anode, the ethanol–CS_2 mixture did not cause apparent carbon deposition and the carbon filaments formation were completely eliminated (Fig. 2b).

In fact, it was well-documented that referring to the interaction between Ni and H_2S at the typical SOFC operating temperature, Ni_3S_2 was thermodynamically more favorable to form than other sulfides via the following reaction [11,18]:

$$3Ni + 2H_2S(g) = Ni_3S_2 + 2H_2(g) \quad \Delta G(850\,^\circ C) = -96.24\ kJ\ mol^{-1} \tag{1}$$

where the thermodynamic data were obtained from HSC 5.0 software and the reaction equilibrium constant $K = 2.992 \times 10^4$. Thus, it could be calculated that Ni_3S_2 would not be produced until the H_2S

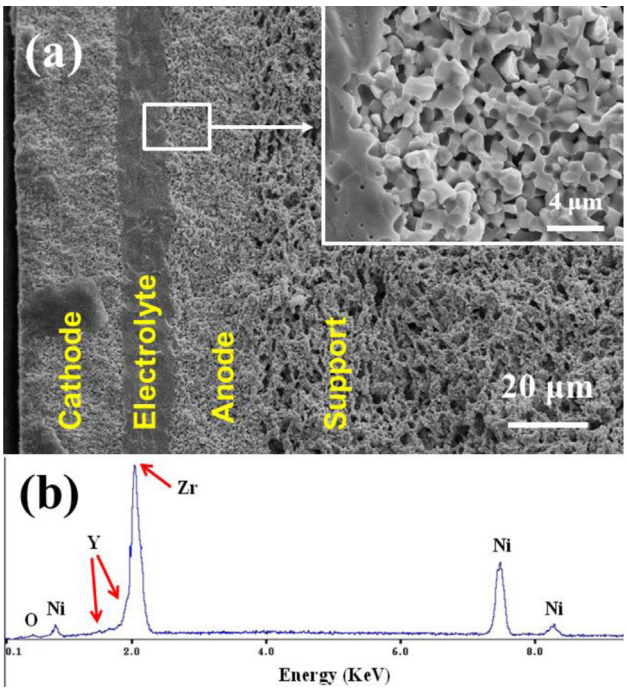

Fig. 1. SEM/EDX results of Ni–S_x cell (a) SEM cross-sectional image of Ni–S_x cell, (b) EDS elemental spectrum of the overall anode of Ni–S_x cell.

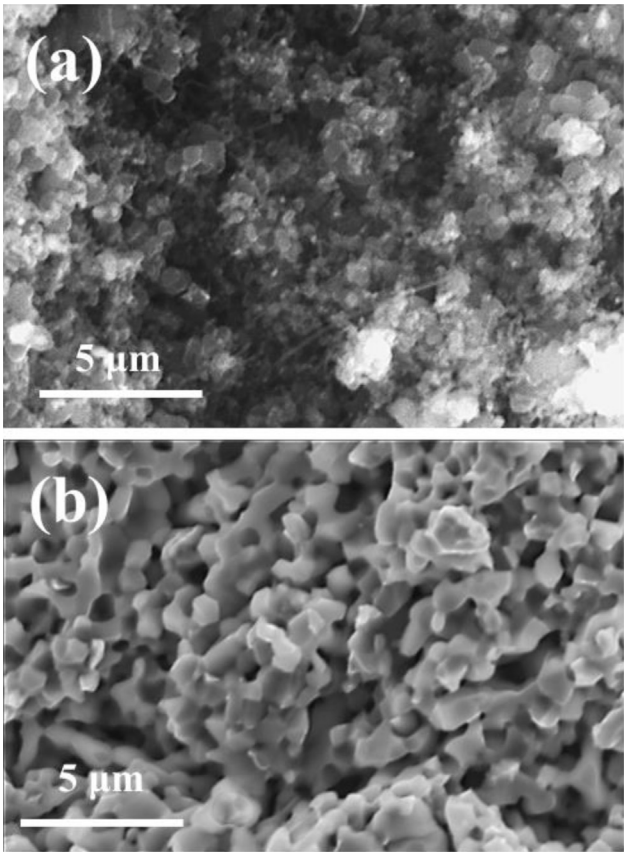

Fig. 2. Anode morphology variation of (a) fresh Ni cell anode after 30 min operation in ethanol at 850 °C, (b) Ni–S_x cell anode after 30 min operation in ethanol at 850 °C.

concentration in H_2–H_2S mixture exceeded 5000 ppm which was substantially higher than that in the present experiment. This observation was also confirmed by researchers in other related work [11,18].

The detailed surface information was revealed through the XPS analysis. Because Ni 2p spectra of metallic Ni in all samples had strong signals which did not change apparently and the surface content of S species was low, both factors could make it more difficult in obtaining accurate deconvolution and fitting. Therefore, the S 2p spectra were examined instead. On the H_2S treated cell in Fig. 3, the peak with a binding energy of 162.07 eV could be assigned to the monolayer of S chemisorbed on Ni surface denoted as S/Ni [19]. At 163.7 eV, the peak was corresponded to the elemental S on either YSZ or Ni–S_x surface [20]. There was another strong peak between 168 eV and 170 eV, which was widely accepted as the sulfate species. Their formation could be ascribed to the interaction of S with oxygen ions during SOFC operation or with the moisture and O_2 when the sample was exposed to the ambient air. After operating in ethanol–CS_2 fuel at 850 °C for 30 min, there was no apparent change in the spectrum. However, the intensity of the peaks decreased, which was mainly caused by the S removal effect of the steam [21].

The C 1s spectrum also provided useful information about the carbon deposition on the studied anode catalyst. In comparison of the overall peak intensity in Fig. 4 between the fresh Ni cell and the Ni–S_x cell after running in ethanol fuel for 30 min at 850 °C, the fresh Ni cell had a much stronger C peak suggesting severer coke formation. At the binding energy of 285.0 eV, the peak was usually associated with C–C or C–H bonds, such as the compound of graphite and CH_x. A smaller fitted curve at 286.6 ± 0.2 eV was assigned to C–O bonds and the peak with the highest binding energy existing between 288 eV and 289 eV was likely to be related with C=O bonds, both of which were associated with complex hydrocarbons [22]. In the Ni–S_x cell, in addition to the C–C/C–H peak with a lower intensity, the peaks corresponding to the C–O and C=O bonds became much less significant, which implied that the chemisorbed S on Ni was not only able to reduce the amount of deposited carbon but also to be influential on the type of coke formed.

3.2. Flow rate determination in ethanol SOFC

Fig. 5 demonstrates a typical performance profile of direct ethanol SOFC using the fresh Ni catalyst without being H_2S-treated. A maximum power density of 704 mW cm^{-2} has been achieved with a 10 mL min^{-1} purge gas flow rate. When the flow rate was adjusted to 5 mL min^{-1} which promised to increase the fuel utilization and alleviate coke formation in SOFC [7], the OCV dropped to 0.8 V while the maximum power density decreased to below 300 mW cm^{-2} since insufficient fuel was provided to the SOFC.

However, when the N_2 flow rate rose up to 20 mL min^{-1}, the button cell performance also degraded slightly despite the fact that

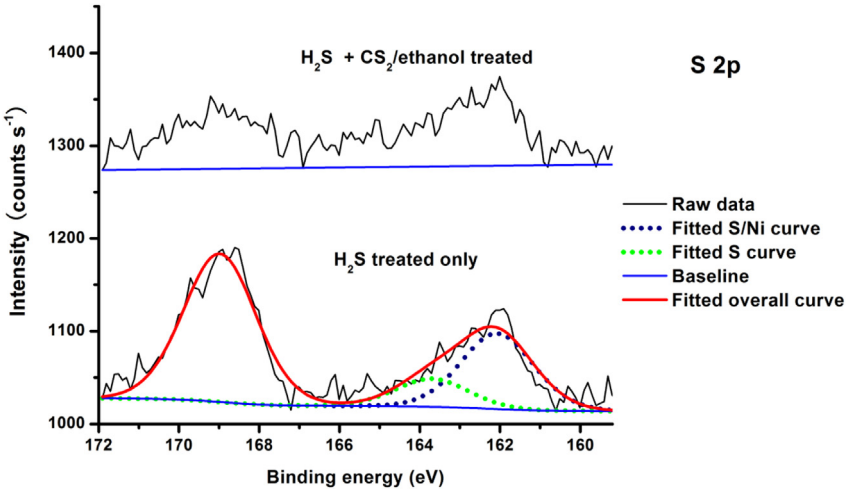

Fig. 3. XPS spectra of S 2p on Ni–S_x anode before and after 30 min operation in ethanol-CS_2 fuels at 850 °C.

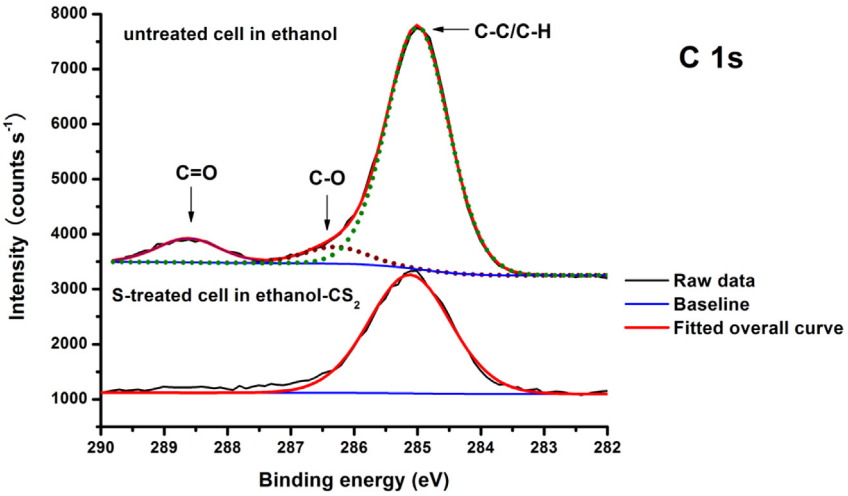

Fig. 4. XPS spectra of C 1s on Ni–S_x and fresh Ni anode, after 30 min operation in ethanol fuels.

its OCV was enhanced to 0.99 V achieved from the higher fuel concentration in the anode chamber. Eventually, when the flow rate was 20 mL min^{-1}, both the ethanol and water vapors in the feed were more over-saturated than that with a lower flow rate. Consequently, they inevitably suffered severer condensation in the fuel supply pipeline where the formed liquid droplets hindered the fuel flow continuity. Therefore, the fuel supply became intermittent, which undermined the SOFC performance and led to the abnormal fluctuation of the *I–V* curve in the figure. In the following experiment, the N_2 flow rate was fixed at 10 mL min^{-1} to stabilize the *I–V* curve.

3.3. Performance of Ni–S_x anode in ethanol-CS_2 fuel

Fig. 6 compares the *I–V* and power density profiles of fresh Ni and Ni–S_x cell fed by the previously specified ethanol fuels at 850 °C. The conventional fresh Ni cell was drastically deteriorated by the coke. The maximum power density degraded to less than 40 mW cm^{-2} from the original 704 mW cm^{-2} and the OCV decreased to 0.7 V. This could be explained by the Ni metal dusting mechanism: the dissolved carbon in Ni lattice caused the volume expansion and the fuel cell structural disintegration. In contrast, the Ni–S_x cell exhibited higher tolerance of coke by sustaining a 400 mW cm^{-2} maximum power density which was essentially identical with the original performance.

The electrochemical impedance spectra were given in Fig. 7. After 2 h of H_2S treatment, the polarization resistance of the cell in H_2 increased from 0.27 Ω cm^2 to 0.41 Ω cm^2 while that in ethanol fuels doubled from ~0.6 Ω cm^2 to ~1.2 Ω cm^2, confirming that the chemisorbed S incompletely deactivated the Ni in terms of the activation/conversion of H_2 and ethanol high temperature derivatives. Nevertheless, the ohmic resistance did not vary substantially. After running in ethanol fuels for 30 min, both the ohmic resistance and the polarization resistance of the fresh Ni cell increased considerably. The former increase proved that the anode physical structure (Ni percolation) was damaged while the latter variation implied the strong catalyst deactivation by coke. In the Ni–S_x cell, however, only the polarization resistance rose up slightly, which was attributable to the limited carbon deposits formed on the anode surface (Fig. 8).

Finally, the cell was working under potentiostatic mode at 0.8 V to evaluate the performances during a longevity test at 850 °C, and the data are shown in Fig. 7. Within 15 min of test, the cell equipped with a fresh Ni anode degraded rapidly to a terminal current density of 0 mA cm^{-2}. On the other hand, the Ni–S_x cell survived for more than 3 h and the total power output, the value corresponding

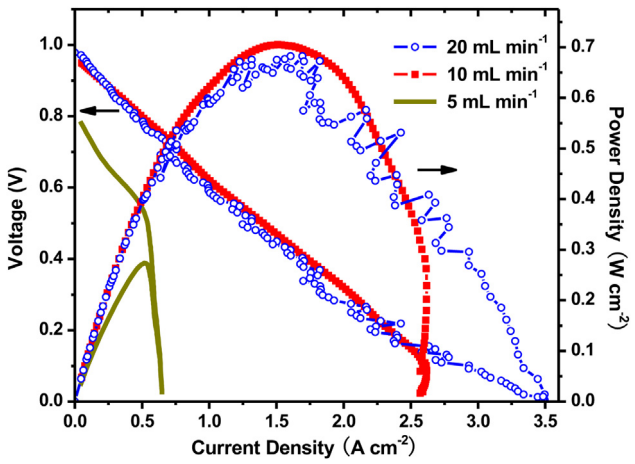

Fig. 5. The influence of carrier gas flow rate on *I–V* and power density profiles at 850 °C for the cell fueled by ethanol.

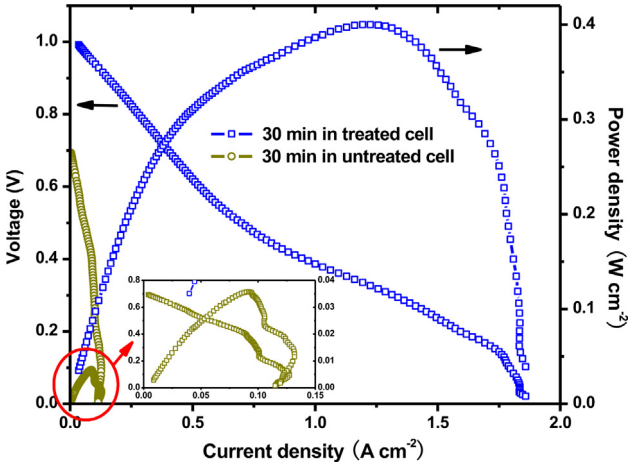

Fig. 6. *I–V* and power density profiles of Ni–S_x cell and fresh Ni cell after 30 min operation in ethanol at 850 °C.

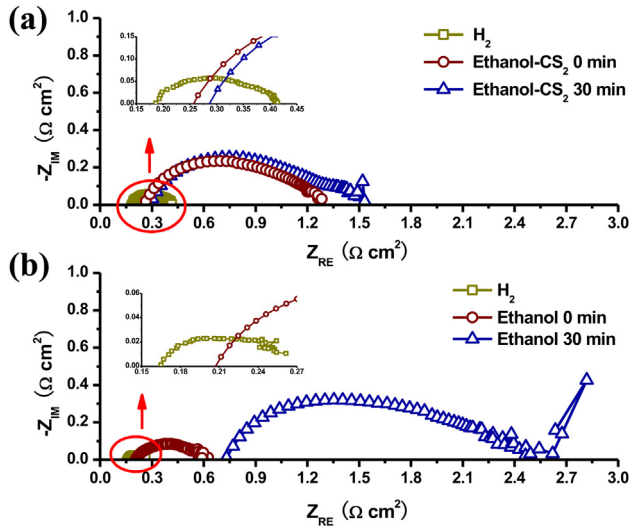

Fig. 7. Electrochemical impedance spectra of (a) Ni–S_x cell and (b) fresh Ni cell, operating in various fuels at 850 °C.

to the area below the signal in the figure, was dramatically higher than that of the fresh Ni cell. Additionally, the escalated degree of the current fluctuation in the S-treated cell was linked with the accumulated water residing in the anode effluent line.

From the comparison, it could be concluded that the Ni–S_x anode catalyst had an improved coke resistance. On fresh Ni anode after ethanol treatment, graphite and a variety of hydrocarbons with complex composition were formed as indicated by the XPS results in Fig. 4. In the meantime, the carbon deposits dissolved into Ni lattice at elevated temperature and continued to grow. The induced internal stress within the Ni matrix was able to disintegrate the whole structure into pieces or even powders [14,23]. This process was illustrated in Fig. 9a. In Ni–S_x cells, the Ni–S_x surface functionally and mechanically protected the anode. Firstly, the reduced activity of Ni–S_x decreased the amount of carbon formed catalytically [13,15]. From another perspective of view, the deposited carbon was more difficult to grow inward to the Ni lattice. Eventually, the chemisorbed S was reported to be able to suppress

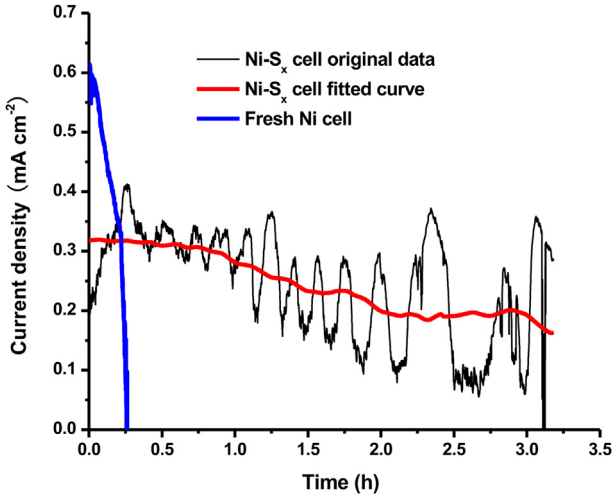

Fig. 8. Performance comparison of Ni–S_x cell and fresh Ni cell operating under potentiostatic mode with applied voltages of 0.8 V at 850 °C.

the carbon transfer, segregation and the graphite nucleation, which finally retarded the metal dusting [14].

In order to prove alleviated metal dusting effect on Ni–S_x catalyst from a microscopic point of view, it became necessary to prevent excess carbon deposits which hindered the observation of microstructure change during metal dusting. Herein, pure CO was selected as the carbon source which was able to induce Ni metal dusting while not causing server coking problem. Ni foam, instead of Ni–YSZ cermet was used as the specimen as it has a complex 3-D structure analogous with Ni anode. Identical H_2S treatment was carried out to prepare Ni–S_x layer on Ni foam surface.

After 24 h treatment in CO at 850 °C, it could be found on fresh Ni sample (Fig. 10a), many dark island-shaped patterns were uniformly distributed across the surface. A higher resolution image in Fig 10b shows they were basically Ni gains as the grain boundaries were still clearly identified. However, on Ni–S_x sample in Fig 10c, there was no apparent change on the surface. Fig. 11 is the EDX spectra of local spots in Fig. 10b, which implied that on the dark island area, there was a considerable amount of carbon whereas on the regular area, only Ni was detected. This revealed that the carbon was dissolved in Ni lattice and metal dusting had occurred. It should be noted that the results of the overall scan of Ni–S_x catalyst in Fig. 1b did not show any carbon existence. Accordingly, it is rational to conclude that Ni–S_x surface layer was capable of alleviating Ni metal dusting problem.

Unfortunately, ethanol molecules were inevitably thermal-cracked at 850 °C with a high reaction rate, which could result in significant coking problems [24]. An equilibrium composition of ethanol at elevated temperature is shown in Fig. 12. Thermodynamically, ethanol was unstable at all the examined temperatures and could decompose into a large amount of C. The stress originated from the gradual carbon accumulation within the porous anode could also cause catastrophic cell failure.

3.4. Optimized stability test

To address the coking issues caused by ethanol thermal cracking, an optimized stability test has been designed. Although the calculated equilibrium composition in Fig. 12 suggested that the higher operation temperature could intensify the coking effect, in practice, a higher temperature usually promoted the thermal decomposition rate of hydrocarbons whereas lowering the temperature was beneficial in balancing the coke form–remove equilibrium. Table 1 describes the measured hydrocarbon composition of anode fuel effluent. Relative to that at 850 °C, the concentration of C_2H_4/C_2H_6 and ethanol increased apparently at 750 °C, whereas the concentration of the rest of the carbon source did not vary significantly, meaning that a higher percentage of the excess anode fuel was able to flow through the anode chamber without being cracked into coke. From an analogous comparison of the fresh Ni cell and the Ni–S_x cell effluent compositions at the same specified temperature, it could be concluded that the chemisorbed S on Ni surface not only alleviated the Ni metal dusting effects as discussed previously, but also was capable of reducing the coke formation rate.

Hence, an optimized stability test was conducted at 750 °C with an applied voltage of 0.8 V (Fig. 13). The conventional cell with a Ni anode still degraded drastically within 4 h. However, a stable power output of approximately 84 mW cm^{-2} was maintained for 22 h until the fuel bubbler drained. Figs. 14 and 15 compared the Ni–S_x cell performance before and after longevity test. Essentially, there was no substantial change of either maximum power density or polarization resistance. However, it was observed that the performance was slightly increased as a function of operating time. Through the analysis of the impedance spectra in Fig 15, it could be

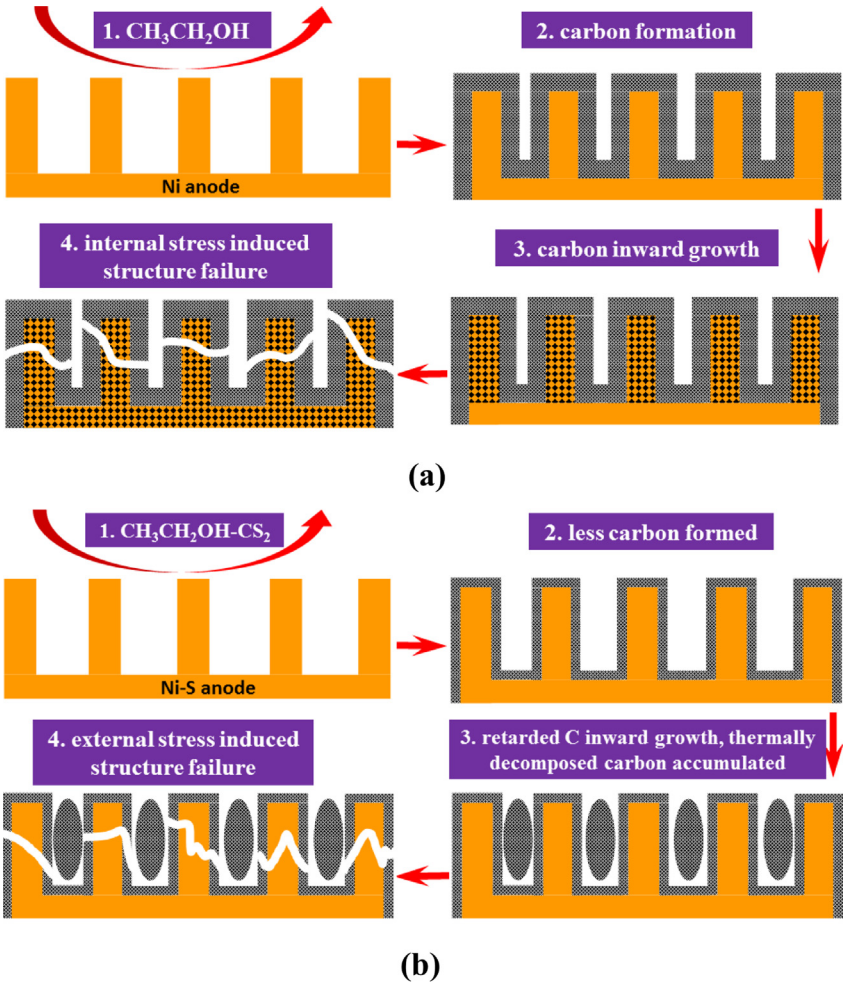

Fig. 9. Schematics of the fuel cell coking-induced failure mechanism in ethanol fuel with (a) fresh Ni anode and (b) Ni–S_x anode operating at 850 °C.

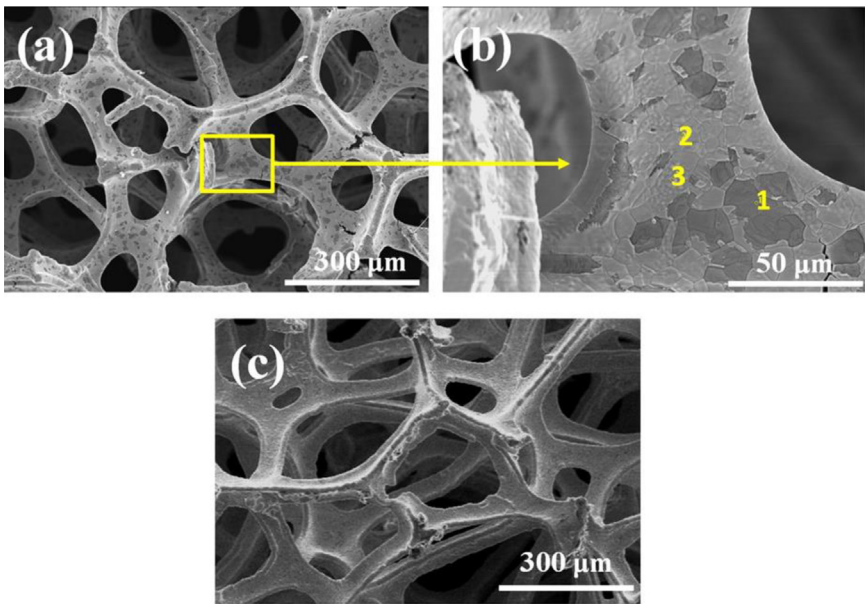

Fig. 10. SEM images (a) fresh Ni foam, (b) magnified view of the boxed area in (a) and (c) H_2S treated Ni foam, after CO exposure for 24 h at 850 °C.

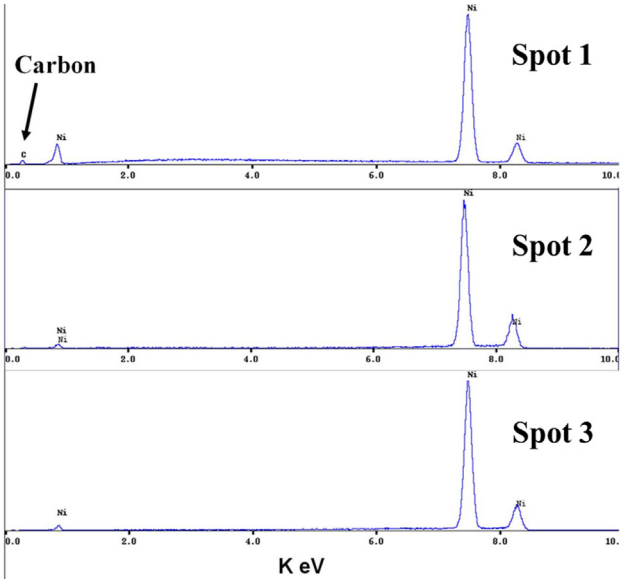

Fig. 11. EDX spectra of local spots in Fig. 10b at Spot 1, Spot 2 and Spot 3.

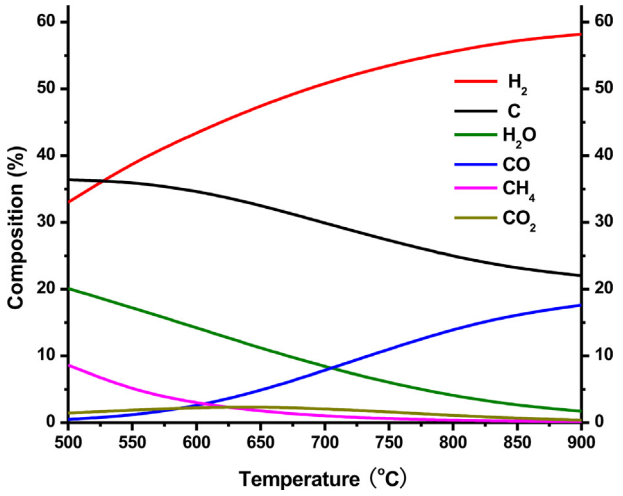

Fig. 12. Calculated composition equilibrium of ethanol thermal decomposition at various temperatures.

seen that the radius of the arc at the high frequency region, which was usually related with anodic process, declined after stability test. This implied higher rate of electrochemical reaction was able to proceed on the anode. Consequently, the performance enhancement was likely to be ascribed to the reversible S removal on Ni anode, although it was not preferred in terms of cell durability in ethanol.

Table 1
The hydrocarbons compositions of anode fuel effluent in fresh Ni cell and Ni–S_x cell. Contribution of N_2 was not considered.

	Ni		Ni–S_x	
	750 °C	850 °C	750 °C	850 °C
CO/CO_2	28.1%	32.8%	27.5%	32.3%
CH_4	18.3%	23.5%	10.7%	18.6%
C_2H_4/C_2H_6	18.5%	10.3%	25.1%	16.6%
CH_3CH_2OH	2.1%	0%	5.9%	0%

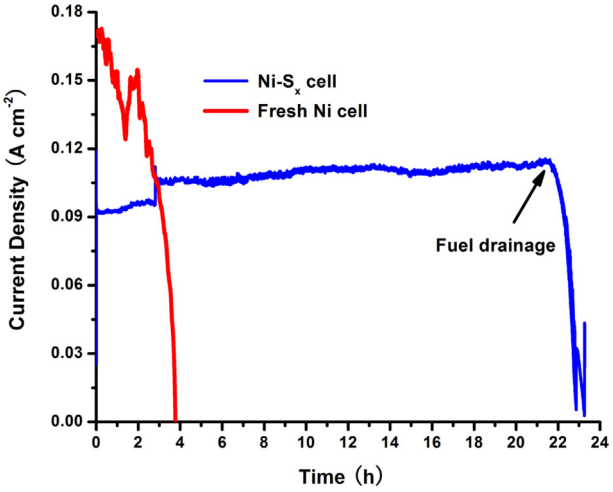

Fig. 13. Optimized stability test of fresh Ni and Ni–S_x cell will applied voltages of 0.8 V at 750 °C.

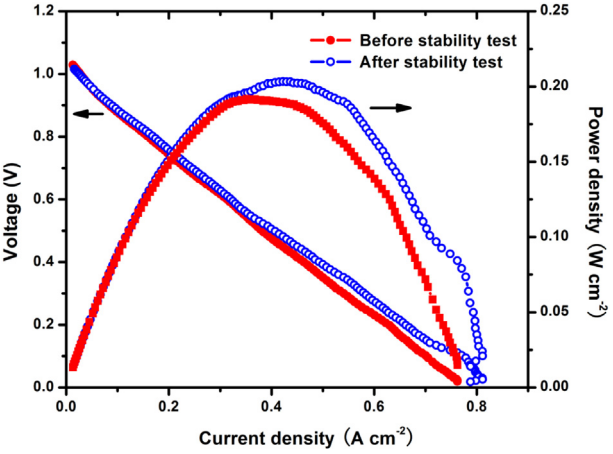

Fig. 14. *I–V* and power density profiles of Ni–S_x cell before and after stability test in ethanol–CS_2 at 750 °C.

4. Conclusion

In this study, the coking resistance of anode supported SOFC was improved by using the Ni–S_x catalyst obtained via *in-situ* H_2S treatment. The resulted characterizations revealed that a combination of S-atom monolayer on Ni surface and the elemental S

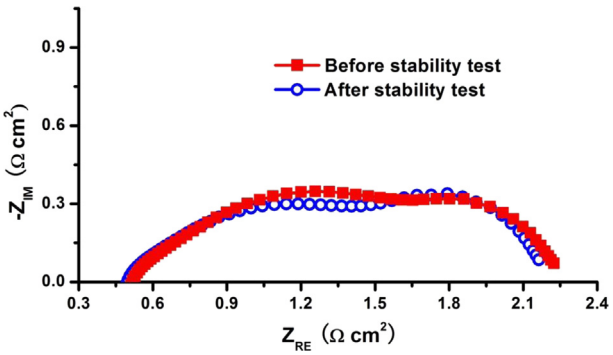

Fig. 15. Electrochemical impedance spectra of Ni–S_x cell before and after stability test in ethanol–CS_2 at 750 °C.

could significantly reduce the coke formation rate on Ni and protect Ni structure against detrimental metal dusting effect. A maximum power density of ~400 mW cm^{-2} has been achieved at 850 °C in ethanol fuel and the cell operated stably for more than 22 h at 750 °C in the identical feed stream.

Since the boiling point of CS_2 (46.3 °C) is lower than that of ethanol (78.4 °C), which is not ideal in maintaining a stable S coverage on Ni, the study of alternative S sources in the future work may promote the coke resistance.

Acknowledgment

Financial support from Natural Sciences and Engineering Research Council (NSERC) of Canada Strategic Project Grant is gratefully acknowledged.

References

[1] S. Park, J.M. Vohs, R.J. Gorte, Nature 404 (2000) 265–267.
[2] S.W. Tao, J.T.S. Irvine, Nat. Mater. 2 (2003) 320–323.
[3] L. Yang, S.Z. Wang, K. Blinn, M.F. Liu, Z. Liu, Z. Cheng, M.L. Liu, Science 326 (2009) 126–129.
[4] B. Huang, S.R. Wang, R.Z. Liu, T.L. Wen, J. Power Sources 167 (2007) 288–294.
[5] S.D. Nobrega, M.V. Galesco, K. Girona, D.Z. de Florio, M.C. Steil, S. Georges, F.C. Fonseca, J. Power Sources 213 (2012) 156–159.
[6] A. Arpornwichanop, N. Chalermpanchai, Y. Patcharavorachot, S. Assabumrungrat, M. Tade, Int. J. Hydrogen Energy 34 (2009) 7780–7788.
[7] M. Cimenti, J.M. Hill, J. Power Sources 186 (2009) 377–384.
[8] H. Kan, Hyunjoo Lee, Appl. Catal. B. Environ. 97 (2010) 108–114.
[9] W. Kobsiriphat, B.D. Madsen, Y. Wang, L.D. Marks, S.A. Barnett, Solid State Ionics 180 (2009) 257–264.
[10] Y.H. Huang, R.I. Dass, J.C. Denyszyn, J.B. Goodenough, Electrochem. Commun. 9 (2007) 1881–1885.
[11] L. Yang, Z. Cheng, M.L. Liu, W. Lane, Energy Environ. Sci. 3 (2010) 1804–1809.
[12] J.P. Trembly, A.I. Marquez, T.R. Ohrn, D.J. Bayless, J. Power Sources 158 (2006) 263–273.
[13] J.R. Rostrupnielsen, J. Catal. 85 (1984) 31–43.
[14] A. Schneider, H.J. Grabke, Mater. Corros. 54 (2003) 793–798.
[15] N. Lakshminarayanan, U.S. Ozkan, Appl. Catal. A. Gen. 393 (2011) 138–145.
[16] N. Yan, X.Z. Fu, J.L. Luo, K.T. Chuang, A.R. Sanger, J. Power Sources 198 (2012) 164–169.
[17] Y. Matsuzaki, I. Yasuda, Solid State Ionics 132 (2000) 261–269.
[18] T. Rosenqvist, J. Iron Steel Inst. 176 (1954) 37–57.
[19] D.R. Mullins, D.R. Huntley, S.H. Overbury, Surf. Sci. 323 (1995) L287–L292.
[20] S.R. Kelemen, G.N. George, M.L. Gorbaty, Fuel 69 (1990) 939–944.
[21] Z. Cheng, M.L. Liu, Solid State Ionics 178 (2007) 925–935.
[22] C. Gadois, J. Swiatowska, S. Zanna, P. Marcus, J. Phys. Chem. C 117 (2013) 1297–1307.
[23] H.J. Grabke, Mater. Corros. 49 (1998) 303–308.
[24] M.B. Pomfret, D.A. Steinhurst, J.C. Owrutsky, J. Power Sources 233 (2013) 331–340.